Physics – Uspekhi **58** (5) 455 – 465 (2015)

METHODOLOGICAL NOTES PACS numbers: 79.20.Eb, **81.07. – b**

Mechanisms of direct laser nanostructuring of materials

V Yu Khomich, V A Shmakov

DOI: 10.3367/UFNe.0185.201505c.0489

Contents

1. **Introduction** 455
2. **Nanostructure formation at solid surfaces under the relaxation of temperature stresses caused by laser heating** 456
3. **Nanostructure formation during pulsed-laser-induced solid surface melting** 458
4. **Nanostructure formation kinetics at solid surfaces during their laser-induced melting** 461
5. **Conclusion** 464

References 464

Abstract. In the given paper, recent results on the development of physical mechanisms and theoretical models of direct laser surface nanostructuring are reviewed. Attention is paid to nanosecond lasers, as they are cheaper and simpler in use than pico- and femtosecond lasers, which is important for the development of further applications. The formation of so-called 'nonresonant' structures, whose period is not directly related to the laser radiation wavelength, is considered. Nanostructuring mechanisms for a number of surface modification processes with and without melting are studied. Corresponding experimental illustrations of nanostructures are given for various materials — polymers, metals, ceramics, and diamond films.

Keywords: nanostructuring, laser, surface, melting, vaporization, displacement, thermal stress

1. Introduction

Laser irradiation of solids can form surface nanostructures which largely determine the physical properties of the surface and are of great interest for materials science, physicochemical mechanics, and solid-state physics. Surface nanostructures find many applications in various fields of physics and engineering:

• in electronics and electrical engineering, optics and spectroscopy, and solar power engineering for optimizing electron emission characteristics and the electrical, thermal, radiative and absorbing properties of the materials;

• in the chemical industry to induce the catalytic properties of materials and control surface wettability;

• in the automotive, aerospace, defense, and atomic industries to improve the durability of ceramic and metal materials and devices which operate under extreme corrosion conditions, and to improve the performance of reactive and diesel engines by nanostructuring their walls and decreasing the friction between the contacting parts;

• in stomatology and orthopedics to improve the biocompatibility of implant coatings and prostheses with living tissues;

• in the hydrogen power industry to increase the power of fuel cells by nanostructuring the surface of the electrodes used in them.

Therefore, of great interest is the problem of developing physical fundamentals for new nanostructuring methods. These methods allow the formation of reliefs with characteristic periods of less than 1 μm on the surface of such materials as refractory superhard ceramics, diamond films, metals and alloys, polymers, and biomaterials.

Despite individual cases of successful physical interpretations of the data obtained, the state of the art was very confusing until recently. Noticeable progress can be observed over recent years. General dependences, which control the real structure formation, are starting to be clarified [1–5]. At the current stage, one needs both the accumulation of the experimental experience on the study of the mechanisms and processes of nanostructuring and the development of new theories which would explain these mechanisms [6].

In order to obtain a surface nanostructure with specific periods under laser irradiation, one needs to spatially modulate the intensity distribution of the incident radiation. Usually, for these purposes one uses either masks as templates that are projected onto the surface [7] or surface screening from the incident radiation by micro- and nanoparticles [8–10], or the interference effect between two or more laser beams at the surface or in the bulk [11–13]. The combination of a laser beam and a cantilever of an atomic force microscope can also be applied [14–16], allowing consequently inducing material relief changes in a number of nano-sized surface regions. Unlike electron and ion beam nanostructuring methods (see, for example, papers [17, 18]), laser nanostruc-

V Yu Khomich Institute for Electrophysics and Electric Power, Russian Academy of Sciences, Dvortsovaya nab. 18, 191186 Saint Petersburg, Russian Federation
V A Shmakov Prokhorov General Physics Institute, Russian Academy of Sciences, ul. Vavilova 38, 119991 Moscow, Russian Federation
E-mail: shmakovv@mtu-net.ru

Received 26 January 2015, revised 16 February 2015
Uspekhi Fizicheskikh Nauk **185** (5) 489 – 499 (2015)
DOI: 10.3367/UFNr.0185.201505c.0489
Translated by A L Chekhov; edited by A Radzig

turing does not need the sample and the energy source to be placed in a special vacuum chamber. Moreover, it is not necessary to provide radiation safety for personal [19, 20].

In this article, we consider surface nanostructuring by a single laser beam without employing any masks or an auxiliary atomic-force microscope cantilever, namely, so-called direct laser nanostructuring [21, 22]. This method is assumed to be much easier and more flexible, because using a single laser beam of a small size allows achieving high interaction locality, which corresponds to the size of the beam and its scanning step along the surface. Moreover, the scanning of the surface with a laser beam of a high pulse repetition rate makes it possible to process extended surfaces within the boundaries of any form with a high spatial resolution. In this article, we discuss the possibility of forming surface nanostructures by nanosecond lasers and present the results of studies into the physical mechanisms and on the development of theoretical models for direct laser nanostructuring.

Structures that are formed in the course of laser infusion of solids can be of various morphologies; however, there are some general structural peculiarities, among which are the following:

(1) the transformation of any region in the initial phase into a new phase macroscopically changes the shape of this region, which results in appearing the specific relief at the sample flat surface. The parameters of the macroscopic deformation are specific for each type of transformations;

(2) there is a specific tendency of the crystals formed towards an ordered arrangement.

2. Nanostructure formation at solid surfaces under the relaxation of temperature stresses caused by laser heating

The deformation process for a solid-state material under sufficiently high stress is accompanied by residual strain which is caused by inelastic effects and transformations of the crystal defect structure. The stress relaxation can be localized due to the formation of domains with the new structure (relaxation domains) within the old excited structure [2]. This is associated with a collective behavior of the excited atoms interacting with each other, which causes the relaxation process to be nonlinear. The action of high mechanical strains induced by a laser beam can macroscopically lead to the excitation of a large number of atoms. In the unexcited state, the atom makes thermally activated random jumps between the lattice sites. Being averaged over a macroscopically small time interval (Debye time), the atomic position can be associated with a quite specific lattice site, so in this sense the atom is localized. In the excited state, the atom travels during the Debye time distances on the order of the lattice parameter, so its position, being averaged over the macroscopically small time interval, cannot be associated with a specific lattice site. Such an excited state can relax through the formation of centers of a new unexcited structure — relaxation domains.

Depending on the external action conditions and on the deformation rate, the relaxation domains can be groups of atoms or vacancies, which form, for example, clusters, dislocation loops, and micropores, as well as dislocation and disclination groups, microcracks, etc. Generally, a domain size distribution should be established. We will consider the relaxation process which is realized through the formation of domains of the same size.

Thermodynamic functions can be obtained by building a relevant ensemble which represents the system in the nonequilibrium state. L I Mandelshtam and M A Leontovich [23, 24] realized this idea by including an auxiliary field, which would turn the thermodynamic state into an equilibrium one, without changing its inhomogeneity. The thermodynamic potential Φ in this case has the form

$$\mathrm{d}\Phi = -S\,\mathrm{d}T + \sum_k^{N_1} A_k\,\mathrm{d}a_k + \sum_k^{N_2} x_k\,\mathrm{d}\xi_k\,, \qquad (1)$$

where S is the entropy in the nonequilibrium state; a_k are external parameters determining the state of the body; A_k are generalized forces conjugate to the parameters a_k; ξ_k are internal parameters characterizing the state of the body under specific values of the external parameters a_k and the temperature T; x_k are parameters that define the external field in which the nonequilibrium system discussed would be in an equilibrium state, and N_1 and N_2 are the numbers of internal and external parameters, respectively.

The meaning of the nonequilibrium entropy and nonequilibrium thermodynamic potential lies in the following: the nonequilibrium state of the body is determined by setting the temperature and external and internal parameters (in the equilibrium state, internal parameters are functions of the temperature and external parameters). At the same time, one can choose the external field, such that the given nonequilibrium state of the body, defined by the given internal parameters, would become the equilibrium one.

The instantaneous value of the nonequilibrium entropy — that is, the entropy characterized by the specific values of external and internal parameters, is by definition equal to the entropy of the equilibrium state characterized by the specified values of the state parameters in this external field. The thermodynamic potential of the nonequilibrium state is defined as the thermodynamic potential of the state in such an external field, without which this nonequilibrium state would be the equilibrium one. If one uses this definition, the instantaneous values of the nonequilibrium entropy and the thermodynamic potential satisfy relation (1) and other known statements, such as a decrease in the thermodynamic potential under isothermal processes proceeding without doing work, and an increase in the entropy under adiabatic processes.

The nonequilibrium state of an elastically strained solid body is defined by the temperature T, strain ε_{ik} or stress σ_{ik} tensors, and by the set of auxiliary internal state parameters $\psi_{ik}^{(1)}, \psi_{ik}^{(2)}, \ldots, \psi_{ik}^{(N)}$ characterizing the degree of system's state departure from the equilibrium state for the specified T and ε_{ik}. In this case, the number of state internal parameters $\psi_{ik}^{(\alpha)}$ is such that, together with T and ε_{ik}, they fully define the state of the system. The parameters $\psi_{ik}^{(\alpha)}$ are second-rank tensors. We will call them relaxation tensors.

The rate of the change of the relaxation tensor $\dot{\psi}_{ik}^{(\alpha)}$ can be obtained from the equation wherein the rate of the process linearly depends on the thermodynamic force:

$$\frac{\partial\Phi}{\partial\psi_{ik}^{(\alpha)}} = \sum_\beta h_{iklm}^{(\alpha,\beta)}\dot{\psi}_{lm}^{(\beta)}\,, \qquad (2)$$

or

$$\frac{\partial\Phi}{\partial\psi_{ik}^{(\alpha)}} = \frac{\partial\Omega}{\partial\dot{\psi}_{ik}^{(\alpha)}}\,, \qquad \Omega = \frac{1}{2}\sum_{\alpha,\beta} h_{iklm}^{(\alpha,\beta)}\dot{\psi}_{ik}^{(\alpha)}\dot{\psi}_{lm}^{(\beta)}\,,$$

where Φ is the thermodynamic potential of a unit volume of the deformed solid body, and $h_{iklm}^{(\alpha,\beta)}$ are material constants. The parameters $h_{iklm}^{(\alpha,\beta)}$ are such that the quantity Ω, which characterizes the decrease in the thermodynamic potential per unit time under fixed temperature and strain, is negative. Stationary states are sustainable in this type of equations and can take various spatial forms [25].

In order to analyze the behavior of the deformed solid, one needs to obtain the expression for the thermodynamic potential Φ as an explicit function of T, ε_{ik}, and $\psi_{ik}^{(\alpha)}$. Assuming the temperature to be fixed and quantities ε_{ik}, $\psi_{ik}^{(\alpha)}$ to be small, we will take advantage of a series expansion of Φ up to the fourth-order terms. Since the thermodynamic potential is a scalar quantity, every term in the expansion should also be a scalar:

$$\begin{aligned}\Phi\left(T,\varepsilon_{ik},\psi_{ik}^{(\alpha)}\right) &= F_0(T) + A_{iklm}\varepsilon_{ik}\varepsilon_{lm} + \sum_{\alpha} B_{iklm}^{\alpha}\varepsilon_{ik}\psi_{lm}^{(\alpha)} \\ &+ \sum_{\alpha,\beta} C_{iklm}^{(\alpha,\beta)}\psi_{ik}^{(\alpha)}\psi_{lm}^{(\beta)} + \frac{1}{24}\left(A_{i\ldots s}\varepsilon_{ik}\varepsilon_{lm}\varepsilon_{np}\varepsilon_{rs}\right. \\ &+ 4\sum_{\alpha} B_{i\ldots s}^{\prime(\alpha)}\varepsilon_{ik}\varepsilon_{lm}\varepsilon_{np}\psi_{rs}^{(\alpha)} + 6\sum_{\alpha,\beta} C_{i\ldots s}^{\prime(\alpha,\beta)}\varepsilon_{ik}\varepsilon_{lm}\psi_{np}^{(\alpha)}\psi_{rs}^{(\alpha)} \\ &+ 4\sum_{\alpha,\beta,\gamma} D_{i\ldots s}^{\prime(\alpha,\beta,\gamma)}\varepsilon_{ik}\psi_{lm}^{(\alpha)}\psi_{np}^{(\beta)}\psi_{rs}^{(\gamma)} \\ &+ \left.\sum_{\alpha,\beta,\gamma,\sigma} E_{i\ldots s}^{\prime(\alpha,\beta,\gamma,\sigma)}\psi_{ik}^{(\alpha)}\psi_{lm}^{(\beta)}\psi_{np}^{(\gamma)}\psi_{rs}^{(\sigma)}\right), \end{aligned} \tag{3}$$

where A_{iklm}, B_{iklm}, C_{iklm}, ... etc. are material constants. Here and further, the summation sign for the same subscripts will be omitted, and for the same superscripts will be kept.

In the equilibrium state and under constant ε_{ik}, the potential Φ takes minimum value and is a function of only volume ε_{ll}. Taking this into account, we can rewrite expansion (3) in the following way:

$$\begin{aligned}\Phi\left(T,\varepsilon_{ik},\psi_{ik}^{(\alpha)}\right) &= \frac{k}{2}\left(\varepsilon_{ll}^2 + \varepsilon_{ll}^4\right) + \sum_{\alpha,\beta} C_{iklm}^{(\alpha,\beta)}\psi_{ik}^{(\alpha)}\psi_{lm}^{(\beta)} \\ &+ \sum_{\alpha,\beta,\gamma,\sigma} E_{i\ldots s}^{(\alpha,\beta,\gamma,\sigma)}\psi_{ik}^{(\alpha)}\psi_{lm}^{(\beta)}\psi_{np}^{(\gamma)}\psi_{rs}^{(\sigma)}, \end{aligned} \tag{4}$$

where k is the bulk modulus.

In order to simplify expressions (2) and (4), one needs to introduce 'normal coordinates', similar to the case of describing oscillations in complicated systems. In other words, we need to introduce such new variables which would be linear combinations of the old variables $\psi_{ik}^{(\alpha)}$, so that each of equations (2) and (4) would contain only one of the variables $\psi_{ik}^{(\alpha)}$. By performing a linear transformation [26] of the variables $\psi_{ik}^{(\alpha)}$, we will choose such new $\psi_{ik}^{(\beta)}$ that the positive quadratic forms in expressions (2) and (4) would take the form

$$\frac{\partial\Phi}{\partial\psi_{ik}^{(\alpha)}} = H_{iklm}^{(\alpha)}\dot{\psi}_{lm}^{(\alpha)},$$

$$\begin{aligned}\Phi &= \frac{k}{2}\left(\varepsilon_{ll}^2 + \varepsilon_{ll}^4\right) + \sum_{\alpha} D_{iklm}^{(\alpha)}\psi_{ik}^{\alpha)}\psi_{lm}^{(\alpha)} \\ &+ \sum_{\alpha} F_{iklmnprs}^{(\alpha)}\psi_{ik}^{(\alpha)}\psi_{lm}^{(\alpha)}\psi_{np}^{(\alpha)}\psi_{rs}^{(\alpha)},\end{aligned}$$

while for an isotropic solid material, one obtains

$$\dot{\psi}_{ik}^{(\alpha)} = 2D^{(\alpha)}\psi_{ik}^{(\alpha)} + 4F^{(\alpha)}\left(\psi_{ik}^{(\alpha)}\right)^3, \tag{5}$$

$$\Phi = \frac{k}{2}\left(\varepsilon_{ll}^2 + \varepsilon_{ll}^4\right) + \sum_{\alpha} D^{(\alpha)}\left(\psi_{ik}^{(\alpha)}\right)^2 + \sum_{\alpha} F^{(\alpha)}\left(\psi_{ik}^{(\alpha)}\right)^4. \tag{6}$$

Equations (5) and (6) govern the behavior of the strained solid body in the course of stress relaxation.

In order to determine the constants which are present in equation (5), let us characterize the whole spectrum of relaxation parameters $\psi_{ik}^{(\alpha)}$ by one variable. For this purpose, we choose the residual strain $\varepsilon_{ij}^0(r,t)$ and introduce a mesoscopic relaxation parameter that determines the field of the relaxation process:

$$\varphi_{ik}(r,t) = \frac{1}{V_0}\int_{V_0}\varepsilon_{ik}^0(r,t)\,\mathrm{d}V,$$

where V_0 is the volume over which $\varepsilon_{ik}^0(r,t)$ is averaged. This means that the system considered — a solid material under deformation — can be represented as three simultaneously coexisting phases: a relaxation field described by the parameter $\varphi_{ik}(r,t)$; a stress field $\sigma_{ik}(r,t)$ corresponding to the external load, and relaxation domains with concentration n.

The time dependences of $\varphi_{ik}(r,t)$, $n(r,t)$ and $\sigma_{ik}(r,t)$ are described by a set of nonlinear differential equations:

$$\begin{aligned}\dot{\varphi}_{ik} &= -\kappa\varphi_{ik} + g_1 n, \\ \dot{n} &= -\gamma n + \frac{\varphi_{ik}\sigma_{ik}}{g_2}, \\ \dot{\sigma}_{ik} &= v(\sigma_{ik} - \sigma_0) - g_3\varphi_{ik}n.\end{aligned} \tag{7}$$

Here v, γ, κ, g_1, g_2, g_3 are material constants. The quantity $\sigma_0(r,t)$ is determined by the amount of the external load applied and corresponds to the residual strains left after relaxation. The first terms on the right-hand side of equations (7) describe, respectively, the damping of the relaxation process, the decay of the formed relaxation domains, and the strain relaxation in the linear approximation, when there is no interaction between them. The second terms in all the equations are responsible for appearing the nonlinearity in the relaxation process. In the first equation, it is related to the relaxation field generation due to the formation of the relaxation domains; in the second one, it takes into account the influence of the relaxation field $\varphi_{ik}(r,t)$ and stress field $\sigma_{ik}(r,t)$ on the origin of the relaxation domains, and in the third one it stands for the influence of the relaxation field and relaxation domains on the rate of the stress relaxation.

The rate of the relaxation field change is significantly smaller than the rates of the atomic relaxation processes, which are characterized by the constants γ and v. This allows one to use the adiabatic elimination of fast variables in equations (7). As a result, we obtain relaxation equation (5) with specific constants:

$$\dot{\varphi}_{ik} = A\varphi_{ik} - B\varphi_{ik}^3,$$

where

$$A = \frac{g_1}{g_2\gamma}\left(\sigma_0 - \frac{g_2\gamma}{g_1}\kappa\right), \quad B = \frac{g_1 g_3}{g_2^2}\frac{\sigma_0}{\gamma^2 v}.$$

The above-described approach does not take into account possible spatial fluctuations of the relaxation parameter, which become more important as the external load and the temperature grow. With these fluctuations taken into consideration, the kinetic equation for the relaxation parameter will have the form

$$\dot{\varphi} = A\varphi_{ik} - B\varphi_{ik}^3 + D\Delta\varphi_{ik}\,. \tag{8}$$

Here, D is the atom diffusion coefficient in the region heated. With the diffusion dispersion taken into account, equation (8) will transform into the generalized Ginzburg–Landau equation [27].

For $\sigma_0 < (g_2\gamma/g_1)\,\kappa$, equation (8) has one sustainable solution: $\varphi(r, t) = 0$. If the critical value is excessed, $\sigma_0 \geqslant \sigma_c = (g_2\gamma/g_1)\,\kappa$, new 'coherent' states of the system with a spatial periodicity can be realized. The period of such structures is given by

$$L = \frac{\sigma_0 - \sigma_c}{2\pi\sigma_0}\sqrt{\frac{3}{8}\frac{D}{v}}\,.$$

Let us now estimate the step of the periodic structure forming on the silicon surface under the action of the laser pulse. We will assume that the residual stresses $\sigma_0 = 10^9$ N m^{-2}, $\kappa \approx \gamma \approx v \approx g_1 \approx 10^3$ s^{-1} (as the ones that determine the frequency of the atomic transition from one equilibrium state to another), $g_2 \approx g_3 \approx 10^{10}$ N m^{-2} is the stresses in the relaxation domains, and $D \approx 10^{-8}$ cm^2 s^{-1} is the atomic diffusion coefficient in the heated region of the crystal. In this case, the period will be $L \sim 3$ μm. As σ_0 increases, which corresponds to harder laser irradiation, the period of the structures being formed has to be determined mostly by the diffusion coefficient D and the rate of stress relaxation. In this case, nanostructures with a period of $L \sim 50-100$ nm will be produced.

At the end of this section, it should be noted that throughout the discussion the bulk case was considered. It was also assumed that the formation of periodical structures in the thin subsurface layer leads to the appearance of corresponding structures at the surface.

Summing up, the approach considered allows explaining the formation of nanostructures in solid materials under the irradiation by a strong laser pulse. The mechanism considered can be implemented under conditions which eliminate the melting of the surface and evaporation in the course of laser infusion of solids.

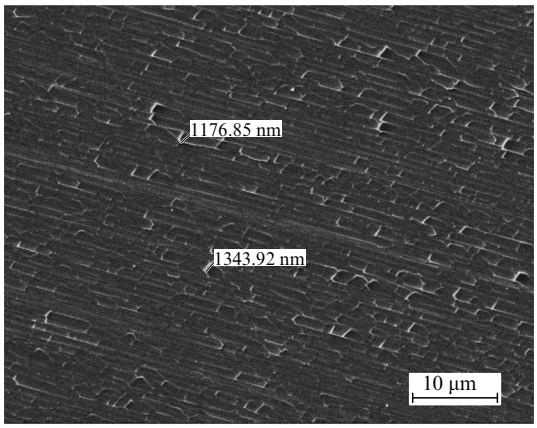

Figure 1. Atomic-force microscopy image of a structure at the surface of zirconium dioxide after irradiation by an ArF laser with a wavelength of 193 nm and energy fluence of 0.14 J cm^{-2}.

Figure 1 depicts a structure formed at the surface of zirconium dioxide (fianite) after laser irradiation [28, 29]. The atomic-force microscopy image shows the surface of a zirconium dioxide plate under irradiation by an excimer nanosecond ArF laser with a wavelength of 193 nm and a fluence per laser pulse of 0.14 J cm^{-2}. The relief analysis allows determining the parameters of the macrodeformation accompanying the structure formation.

3. Nanostructure formation during pulsed-laser-induced solid surface melting

The irradiation of a solid surface by a laser pulse with the specific power Q and duration τ can lead to the melting of the surface layer. Further nucleation of a crystal phase from the melt can be of a fluctuation or spontaneous character, depending on the supercooling degree. In this case, a supercooled state of the melt can arise due to the high rate of the heat transfer to the bulk of the solid phase, so a significant temperature drop can form on the interface between liquid and solid.

Fluctuation nucleation occurs under weak supersaturation (supercooling), when the size of the critical nucleus significantly exceeds the lattice constant. The rate of a new phase formation in the classical Zeldovich–Frenkel nucleation theory is determined by the number of critical nuclei that form in the unit volume per unit time [30]. Spontaneous nucleation takes place under significantly high cooling rates, for which the corresponding time that it takes to reach the supercooled state is significantly smaller than the fluctuation nucleation time.

If a crystal phase nucleus consisting of n atoms is formed from the melt, the change of thermodynamic potential is expressed as

$$\Delta\Phi(n) = (\mu_2 - \mu_1)(n_1 + n_s) + 4\pi r^2\sigma\,,$$

where μ_1 and μ_2 are chemical potentials of the atoms in the solid and liquid phases, respectively, $n = n_1 + n_s$, $n_1 = 4\pi r^3/3a^3$ is the number of atoms inside the nucleation center of the crystal phase, $n_s = 4\pi r^2/a^2$ is the number of atoms at the surface of the nucleation center of the crystal phase, a is the elementary cell size, r is the radius of the nucleation center of the crystal phase, and σ is the surface tension coefficient. The critical size of the new phase, $r^* = 2[\sigma a^3(\mu_1 - \mu_2)^{-1} - a]$, can be obtained from the equation $\partial\Delta\Phi/\partial r = 0$. For low supercooling degree, when $\sigma a^3(\mu_1 - \mu_2)^{-1} - a \gg 1$, the nucleation shows a fluctuation character. The new phase in this case forms from a critical nucleus, whose size r^* significantly exceeds the lattice constant (Fig. 2, curve *1*). The existence of a subcritical region allows considering a metastable state and, consequently, introducing an equilibrium distribution function under supercooling conditions.

During spontaneous nucleation, which takes place under strong supercooling, when $\sigma a^3(\mu_1 - \mu_2)^{-1} - a \leqslant 1$, the critical radius of the new phase nucleation center does not exceed the atomic size. In this case, the initial phase can be considered to be absolutely unstable. It follows that the thermodynamic potential $\Delta\Phi(n) \approx (\mu_2 - \mu_1)(n_1 + n_s)$ smoothly decreases as r increases (curve *2* in Fig. 2). There is no need to introduce here

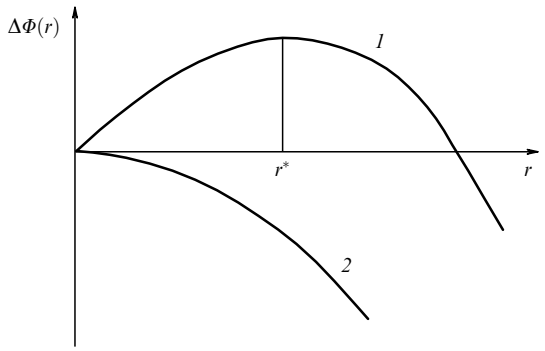

Figure 2. Free energy of the system versus the sizes of the formed crystal phase nucleation centers: *1* — fluctuation nucleation, and *2* — spontaneous nucleation.

the parameter σ, since the bulk change of the thermodynamic potential exceeds the surface one for any size of the new phase nucleation centers.

It should also be noted that the surface energy in the case of the liquid–gas interface is expressed in the form $E = -(1/2)\, z\varepsilon_{AA} n_s$. Here, z is the coordination number, and ε_{AA} is the potential energy of the interaction between the two closest molecules in the liquid. The interaction energy between surface molecules of a liquid with gas molecules can be neglected due to the relatively small gas density. In the case of solid phase formation (B atoms) from the liquid one, the surface energy is given by

$$E^1 = n_s \left[z\varepsilon_{AB} - \frac{1}{2}\, z(\varepsilon_{AA} + \varepsilon_{BB}) \right]$$

and $E^1 < E$, because the potential interaction energy $\varepsilon_{AB} < 0$. Therefore, the surface tension coefficient of the liquid–solid interface is significantly smaller than that for the liquid–gas system. This means that spontaneous nucleation is more likely to take place under liquid–solid phase transitions than under liquid–gas ones.

Let a heat flux with density $q(x, t)$ fall on the surface of a solid approximated by a half-space. The power carried by the flux is such that a solid–liquid phase transition takes place. The temperature fields in liquid $[T_1(x, t)]$ and solid $[T_2(x, t)]$ phases are described by heat conduction equations with corresponding boundary conditions:

$$\frac{\partial^2 T_1}{\partial x^2} = \frac{1}{a_1} \frac{\partial T_1}{\partial t}\,, \quad 0 < x < y(t)\,, \tag{9}$$

$$\frac{\partial^2 T_2}{\partial x^2} = \frac{1}{a_2} \frac{\partial T_2}{\partial t}\,, \quad y(t) < x < \infty\,, \tag{10}$$

$$T_2(x, 0) = T_2(\infty, t) = T_{in}\,, \tag{11}$$

$$\frac{\partial Q(t)}{\partial t} = -\lambda \left.\frac{\partial T_1}{\partial x}\right|_{x=0}\,, \tag{12}$$

$$\left.T_1\right|_{x=y(t)} = \left.T_2\right|_{x=y(t)} = T_{tr}\,, \tag{13}$$

where $y(t)$ is the coordinate of the moving boundary of the phase transition, $a = \lambda/c\rho$, λ, c are, respectively, thermal diffusivity, thermal conductivity, and heat capacity of the metal unit volume, ρ is the material density, $Q(t)$ is the absorbed energy per unit surface area in time $t < \tau$, τ is the pulse duration, T_{tr} is the phase transition temperature, and T_{in} is the initial temperature. Subscript 1 corresponds to the liquid phase, and subscript 2 to the solid phase. The coordinate x is measured from the surface. The latent heat of the transition H is supplied through the liquid phase and is absorbed at the moving front of the phase transition:

$$\lambda_1 \left(\frac{\partial T_1}{\partial x} \right)\bigg|_{x=y(t)} = H\rho \frac{dy}{dt} + \lambda_2 \left(\frac{\partial T_2}{\partial x} \right)\bigg|_{x=y(t)}\,. \tag{14}$$

In order to simplify the problem, we will replace boundary condition (12) with the following one:

$$T_1(0, t) = T_0 = T_1(0, \tau) > T_{tr}\,, \tag{15}$$

where T_0 is the temperature of the melted metal at the surface, which can be obtained from the heat balance equation

$$Q(\tau) = H\rho y(\tau) + \int_0^{y(\tau)} C_2\rho(T_{tr} - T_{in})\, dx + \int_0^{y(\tau)} C_1\rho(T_1 - T_{tr})\, dx + \int_{y(\tau)}^{\infty} C_2\rho(T_2 - T_{in})\, dx\,. \tag{16}$$

It is possible to correctly formulate the problem by equations (9)–(13), with Eqn (12) being replaced by Eqn (15), if the temperature of the sample surface reaches the phase transition temperature,

$$T(t_0) = T_{tr}\,, \tag{17}$$

in a time $t_0 \ll \tau$ and, during the further process for $t_0 < t < \tau$, the liquid phase temperature changes insignificantly:

$$\frac{T(\tau) - T_{tr}}{T_{tr}} \ll 1\,. \tag{18}$$

The limitations put on the radiation characteristics due to conditions (17) and (18) will be discussed below.

The solutions of equations (9), (10) with boundary conditions (11), (13), (15) have the form

$$T_1 = T_0 + (T_{tr} - T_0)\, \frac{\operatorname{erf}(u/\sqrt{2a_1})}{\operatorname{erf}(\beta/\sqrt{2a_1})}\,,$$

$$T_2 = T_{in} - (T_{in} - T_{tr})\, \frac{\operatorname{erfc}(u/\sqrt{2a_2})}{\operatorname{erfc}(\beta/\sqrt{2a_2})}\,, \tag{19}$$

where $u = x/\sqrt{2t}$, $y(t) = \beta/\sqrt{2t}$, and β is some constant. Availing oneself of expressions (19) and taking the integrals in the thermal balance equation (16), after appropriate transformations we obtain

$$T_0 = T_{tr} + \left\{ \frac{Q(\tau)}{\sqrt{\tau}} - \sqrt{2}\, H\rho\beta - 2C_2\rho(T_{tr} - T_{in}) \times \left[\sqrt{a_2} \exp\left(-\frac{\beta^2}{2a_2} \right) \right] \left[\sqrt{\pi} \operatorname{erfc}\left(\frac{\beta}{\sqrt{2a_2}} \right) \right]^{-1} \right\} \times \left\{ 2C_1\rho\sqrt{a_1} \left[1 - \exp\left(-\frac{\beta^2}{2a_1} \right) \right] \left[\sqrt{\pi} \operatorname{erf}\left(\frac{\beta}{\sqrt{2a_1}} \right) \right]^{-1} \right\}^{-1}. \tag{20}$$

The quantity β, which characterizes the speed of phase boundary motion, can be found from equation (14). Assuming $a_1 = a_2$ and substituting Eqns (19) and (20) into Eqn (14),

we arrive at a transcendent equation for β:

$$2c\rho(T_{\rm tr}-T_{\rm in})\sqrt{\frac{a}{\pi}} = \left\{\sqrt{2}\,H\rho\beta\left[\exp\left(\frac{\beta^2}{2a}\right)-2\right]+\frac{Q(\tau)}{\tau}\right\}\operatorname{erfc}\frac{\beta}{\sqrt{2a}}\,. \quad (21)$$

Solving equation (14) allows calculating the melting depth for various materials under their irradiation by laser pulses with various durations and power.

After the laser pulse infusion ends, the liquid phase starts the transition into the solid phase. The cooling rate in our case will be maximum if, first, the amount of heat absorbed by the solid phase during the pulse action is small in comparison with the energy spent on the formation of the liquid layer and, second, the liquid phase superheating turns out to be weak: $(T_0-T_{\rm tr})/T_{\rm tr}\ll 1$. The requirement that liquid phase superheating be small can be fulfilled under specified laser energy fluence for sufficiently short pulses, so that the melting depth is small. For example, in the case of Cu at $Q(t)=0.5$ J cm^{-2} and $\tau=10^{-8}$ s, the depth of the melted layer is $l=\beta\sqrt{2\tau}\sim 0.2$ μm, and the superheating degree of the liquid phase is $(T_0-T_{\rm tr})/T_{\rm tr}\sim 0.1$.

In order to determine the cooling rate, the problem of melted layer cooling through the heat transfer to the bulk of the solid phase needs to be solved. In this case, the initial temperature distribution is described by expressions (19) for the instant of time when the pulse ends. If the melting depth is small and the liquid phase superheating degree fulfills the condition

$$\frac{T_0-T_{\rm tr}}{T_{\rm tr}}\ll 1\,,$$

then the temperature of the liquid can be assumed constant and equal to $T_{\rm tr}$. We will approximate the nonstationary temperature distribution as

$$T(x,t)=T_{\rm tr}\,\frac{x-\gamma(t)}{b(t)-\gamma(t)}\,,\quad x>b(t),\quad t>0\,, \quad (22)$$

$$T(x,\eta)=\varphi(\eta)\left(1-\frac{x}{\Psi(\eta)}\right),\quad x>0\,. \quad (23)$$

In order to simplify the calculations, we will put $T_{\rm in}=0$. Here, $b(t)$ and $\gamma(t)$ are the laws of motion for temperature boundaries $T=T_{\rm tr}$ and $T=T_{\rm in}=0$. The time η is measured from the instant t_1, when the temperature boundary $T=T_{\rm tr}$ reaches the surface, so t_1 is the solution of the equation $b(t_1)=0$; $\varphi(\eta)$ is the law for the surface temperature change for $t>t_1$, and $\Psi(\eta)$ characterizes the motion of the temperature boundary $T=0$ for $t>t_1$.

The functions $y(t)$, $b(t)$, $\varphi(\eta)$, $\Psi(\eta)$ can be found by applying the variational method (Bio principle) based on introducing the vector field $\mathbf{H}(x,y,z,t)$ into heat conduction equation [31]. Vector field $\mathbf{H}(x,y,z,t)$, known as the thermal displacement, is defined by the equation

$$\dot{\mathbf{H}}=\left(\frac{\partial}{\partial t}\right)\mathbf{H}(x,y,z,t)\,,$$

where $\mathbf{H}$ is the vector representing the local heat flux density.

The energy conservation law and the heat conduction equation have, respectively, the form

$$cT=-\operatorname{div}\mathbf{H}\,,$$
$$\operatorname{grad}T+\left(\frac{1}{\lambda}\right)\mathbf{H}=0\,.$$

By introducing generalized coordinates $\mathbf{H}=\mathbf{H}(q_1,q_2,\ldots,q_n,x,y,z,t)$, we obtain a set of differential equations for the unknown q_i:

$$\frac{\partial V}{\partial q_i}+\frac{\partial D}{\partial q_i}=Q_i\,,$$

where V is the heat potential

$$V=\frac{1}{2}\int cT^2\,{\rm d}V,$$

D is the dissipative function

$$D=\frac{1}{2}\int\left(\frac{\dot{\mathbf{H}}^2}{\lambda}\right){\rm d}V,$$

and Q_i is the generalized external force

$$Q_i=-\int T\,\frac{\partial\dot{\mathbf{H}}}{\partial q_i}\,\mathbf{n}\,{\rm d}S\,.$$

After applying the variational principle, we arrive at

$$\gamma(t)=\beta\sqrt{2\tau}+\alpha+\frac{87}{215}\,\alpha\left[\left(1+\frac{215at}{3\alpha^2}\right)^{1/2}-1\right], \quad (24)$$

$$b(t)=\beta\sqrt{2\tau}-\frac{128}{215}\,\alpha\left[\left(1+\frac{215at}{3\alpha^2}\right)^{1/2}-1\right], \quad (25)$$

$$\varphi(\eta)=T_{\rm tr}\left[1+\frac{80a\eta}{\beta\sqrt{2\tau}+\alpha+(87/215)\,\alpha\bigl(215\beta\sqrt{2\tau}/(128\alpha)+1\bigr)}\right], \quad (26)$$

$$\Psi(\eta)=\left\{\left[\beta\sqrt{2\tau}+\alpha+\frac{87}{215}\,\alpha\left(\frac{215\beta\sqrt{2\tau}}{128\alpha}+1\right)\right]^2+80a\eta\right\}^{1/2}, \quad (27)$$

where $\alpha=\sqrt{\pi a\tau}\,\exp\left[\beta^2/(2a)\right]\operatorname{erfc}\left[\beta/(2a)\right]$.

Crystallization is caused by the appearance and growth of crystal structure nuclei in the melt. The growth rate of the nucleus of a crystal is expressed as [32]

$$\frac{{\rm d}r}{{\rm d}t}=v_0 d\,\exp\left(-\frac{U}{k_{\rm B}T}\right)\left[1-\exp\left(-\frac{\Delta\mu}{k_{\rm B}T}\right)\right], \quad (28)$$

where v_0 is the Debye atomic oscillation frequency in the supercooled liquid, U is the activation energy for the atom displacement, $k_{\rm B}T$ is the thermal energy, d is the characteristic size per atom, $\Delta\mu$ is the difference between the atomic chemical potentials in the supercooled liquid at the temperature T and at the phase transition temperature $T_{\rm tr}$: $\Delta\mu=h(T_{\rm tr}-T)/T_{\rm tr}$, and h is the heat of phase transition per atom.

The characteristic time of nuclei growth is determined as the time after which the sizes of the new phase nucleation centers barely change. In this time, the temperature averaged

over the thickness of the melted layer becomes equal to $T_{tr} - \Delta_0$, where Δ_0 is the supercooling degree under which a new phase nucleus growth actually stops. Therefore, the characteristic time τ_0 can be found from the equation

$$\int \frac{T(x,\tau_0)\,dx}{\beta\sqrt{2\tau}} = T_{tr} - \Delta_0\,, \qquad (29)$$

where $\beta\sqrt{2\tau}$ is the thickness of the melted layer.

In order to determine τ_0 from equation (29), we need to know, besides the temperature distribution specified by formulas (22)–(27), the value of supercooling degree Δ_0. It follows from equation (28) that nucleus growth actually takes place when supercooling $\Delta_0 \ll T_{tr}$. Under stronger supercooling, the growth of the new phase nucleation centers stops. The mobility of the atoms in the supercooled liquid, described by the quantity $\exp(-U/k_B T)$, starts to play an important role here. The average cooling rate of the melt is expressed as $\varepsilon = \Delta_0/\tau_0$, and the change in the temperature averaged over the thickness of the layer takes the form $T(t) = T_{tr} - \varepsilon t$.

By integrating relation (28) and taking into account the fact that $(T_{tr} - T(t))/T_{tr} = \varepsilon t/T \ll 1$ and $h \sim 0.1U$, we obtain the size of the crystal phase nucleus in the supercooled liquid:

$$r(t) = v_0 d \exp\left(-\frac{U}{k_B T_{tr}}\right)\frac{k_B T_{tr}^2}{U\varepsilon} \times\left\{\frac{h}{U+h} - \exp\left(-\frac{U\varepsilon t}{k_B T_{tr}^2}\right) + \frac{U}{U+h}\exp\left[\frac{\varepsilon t(U+h)}{k_B T_{tr}^2}\right]\right\} \approx R\left[1 - \exp\left(-\frac{U\varepsilon t}{k_B T_{tr}^2}\right)\right], \qquad (30)$$

where

$$R = \frac{v_0 d \exp\left[-U/(k_B T_{tr})\right] k_B T_{tr}^2 h}{\varepsilon U(U+h)}\,.$$

The size $r(t)$ of the crystal nucleus tends to its limit value R in the relaxation time $\tau_0 = k_B T_{tr}^2/\varepsilon U$, which, according to the initial definition, is the characteristic time of this process. On the other hand, the characteristic time is connected with the cooling rate by the relation $\tau_0 = \Delta_0/\varepsilon$, where Δ_0 is the supercooling degree, which is included in equation (29); therefore, one has $\Delta_0 = k_B T_{tr}^2/U$. We can now obtain τ_0 from equation (29) and then determine the corresponding cooling rate and the limit size of the new phase nucleus.

It should be noted that the surface energy is neglected in equation (28), because for high cooling rates, $\varepsilon > 10^6$ grad s^{-1}, the characteristic value of the critical nucleus size $r = [2\sigma/(\Delta\mu)\,m]\,d^3$ turns out to be on the order of the interatomic distance [here, $(\Delta\mu)\,m = \int \Delta\mu(t)\,dt/\tau_0$ and σV is the free surface energy per unit area, and V is the volume]. If the cooling rate is high, the bulk change in the thermodynamic potential exceeds that of the surface for any nucleus size.

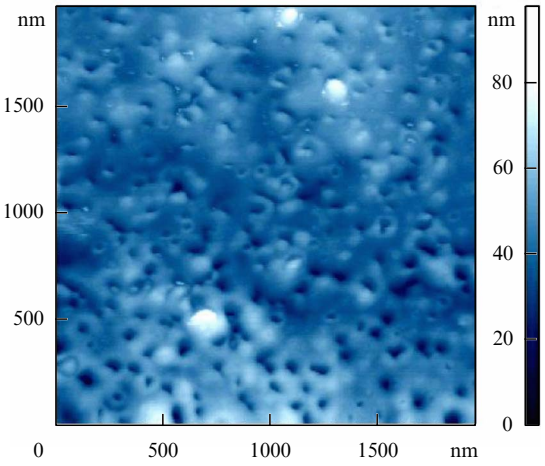

Figure 3. Atomic force microscopy of a stainless steel surface relief after its irradiation by an ArF laser with the wavelength of 193 nm and energy fluence in the spot center of around 4 J cm^{-2} (20 pulses with repetition rate 2 Hz).

In this way, one can calculate the cooling rates and the characteristic sizes of the nuclei that are formed during the cooling of the melted layer [33, 34]. If aluminum is irradiated by a laser pulse with the duration $\tau \sim 10^{-8}$ s, nanostructures with the period of 50 – 100 nm will form at the metal surface after the solidification of the melted region if the absorbed laser pulse energy $Q \approx 0.4$ J cm^{-2}. For the energy $Q \approx 4.4$ J cm^{-2} and pulse length $\tau \approx 10^{-6}$ s, the size of the nanostructures grows up to 500 nm. In the case of the irradiation of a copper surface, in order to obtain nanostructures 50 – 100 nm in size, it is required that $Q \approx 1$ J cm^{-2} and $\tau \approx 10^{-8}$ s. Laser pulse energy $Q \approx 6$ J cm^{-2} and $\tau \approx 10^{-6}$ s are necessary to obtain 100 – 500-nm structures on a silver plate. In accordance with the calculated results, the amount of energy that needs to be absorbed during a pulse with $\tau \approx 10^{-8}$ s for obtaining nanostructures with a size of up to ~ 100 nm at the surfaces of various materials is indicated in Table 1.

Figure 3 shows an image of a stainless steel surface in the melting region after the nanosecond radiation infusion with a wavelength of 193 nm. A relief in the form of pits with a diameter of 25 – 40 nm and a depth of around 40 nm can be seen.

4. Nanostructure formation kinetics at solid surfaces during their laser-induced melting

In Section 3, we estimated and obtained the characteristic sizes of the crystal phase nucleation centers that form during the cooling of a melted surface layer. Let us now determine the size distribution function of the formed nucleation centers under the conditions of spontaneous nucleation [35, 36].

Table 1. Energies absorbed during laser pulse irradiation with length $\tau \approx 10^{-8}$ s as needed for the formation of nanostructures with sizes of up to ~ 100 nm at the surfaces of various materials.

Material	Al	Cu	Au	Ag	Mo	Si_3N_4
Q, J cm^{-2}	0.44 – 0.74	1.02 – 1.88	0.72 – 1.31	0.76 – 1.33	1.26 – 2.4	0.6 – 1.0

In order to derive the kinetic equation for the size distribution function $z(n,t)$ of the nuclei, we will consider the phase space comprising only one axis — an axis of the sizes of new phase centers. There are three points on an axis in this space, which stand for the new phase nucleation centers consisting of $n-1$, n, and $n+1$ atoms, respectively. We will derive an equation that will allow us to find the distribution function $z(n,t)$ of these centers over n. If $P_+(n)$ and $P_-(n)$ are, respectively, the probabilities of an atom attachment and detachment from the region occupied by the new phase per unit time, then four processes are possible:

(1) $z(n,t)\,P_-(n)$; (2) $z(n,t)\,P_+(n,t)$;

(3) $z(n-1,t)\,P_+(n-1)$; (4) $z(n+1,t)\,P_-(n+1)$.

The first and the second processes determine the number of new phase centers transferred from point n to points $n-1$ and $n+1$ in the time $\mathrm{d}t$. The two others determine the number of new phase centers which occur at the point n in the time $\mathrm{d}t$ due to leaving other points. Therefore, the desired equation may be written down as

$$\frac{\mathrm{d}z(n,t)}{\mathrm{d}t} = -z(n,t)\big[P_+(n)+P_-(n)\big] + z(n-1,t)\,P_+(n-1) + z(n+1,t)\,P_-(n+1)\,. \quad (31)$$

The fact that $P_\pm(n)$ does not depend on z and there are no integral terms in equation (31) restricts the consideration by the initial stage of the process. If we assume $n \gg 1$ (which means that we are considering new phase centers which have a specific structure and therefore consist of a significant number of atoms), then after writing down the series expansion of the functions on the right-hand side of equation (31) up to the 2nd-order infinitesimal, we arrive at

$$\frac{\mathrm{d}z(n,t)}{\mathrm{d}t} = \frac{1}{2}\frac{\partial^2}{\partial n^2}\big[z(n,t)\big(P_+(n)+P_-(n)\big)\big] + \frac{\partial}{\partial n}\big[z(n,t)\big(P_-(n)-P_+(n)\big)\big]\,. \quad (32)$$

In our case, the probability is defined as [37]

$$P_\pm(n) = P_0 \exp\left(\pm\frac{1}{2k_\mathrm{B}T}\frac{\mathrm{d}}{\mathrm{d}n}\,\Delta\Phi(n)\right) = P_0(1\pm\varepsilon)\,, \quad (33)$$

where $\varepsilon = 1/(2k_\mathrm{B}T)\,\mathrm{d}\Delta\Phi(n)/\mathrm{d}n$.

By substituting Eqn (33) into Eqn (32), after some transformation we obtain

$$\frac{\partial z(n,t)}{\partial t} = v\exp\left[-\frac{U}{k_\mathrm{B}T(t)}\right] n^{2/3}\left[\frac{\partial^2 z}{\partial n^2} + \frac{1}{k_\mathrm{B}T(t)}\times\frac{\partial}{\partial n}\left(\frac{\mathrm{d}\Delta\Phi(n)}{\mathrm{d}n}\,z(n,t)\right)\right]. \quad (34)$$

Here, v is the Debye frequency, U is the activation energy for the atomic displacement, and $T(t)$ is the time-dependent temperature of the system. Equation (34) is valid under the assumption that the growth happens only due to the joining of single atoms in an activated way over the potential barrier. The driving force of the process under the conditions of spontaneous nucleation is expressed as

$$\frac{\mathrm{d}\Delta\Phi(n)}{\mathrm{d}n} = -h\,\frac{T_0-T(t)}{T_0}\,,$$

where h is the phase transition enthalpy per atom, and T_0 is the melting temperature.

At the initial instant of time there are no nuclei in the system. Therefore, one has

$$z(n,0) = 2N\delta(n-1)\,, \quad (35)$$

where N is the number of particles per unit volume, and $\delta(n-1)$ is the delta function defined in the following way: $\int_1^\infty \delta(n-1)\,\mathrm{d}n = 1/2$. Due to the fact that nucleus growth takes place only for $n>1$, the flux in the size space at $n=1$ is assumed to be zero:

$$\left(\frac{\partial z(n,t)}{\partial n} - \frac{h}{k_\mathrm{B}T}\,\frac{T_0-T(t)}{T_0}\,z(n,t)\right)_{n=1} = 0\,. \quad (36)$$

A natural condition consists in the absence of very large new formations:

$$z(\infty,t) = 0\,. \quad (37)$$

The set of equations (34)–(37) is closed and the time dependence of the temperature in it is a known function; however, an exact solution of this system unlikely exists. We will take advantage of an approximate solution method and estimate the characteristic time of the process, after which the nucleus size change can be neglected.

The rate of the change in the nucleation center radius can be written down in the form of expression (28):

$$\frac{\partial r}{\partial t} = va\exp\left(-\frac{U}{k_\mathrm{B}T}\right)\left[1-\exp\left(-\frac{\Delta\mu}{k_\mathrm{B}T}\right)\right]. \quad (38)$$

Here, a is the elementary cell size, and $\Delta\mu = h(T_0-T)/T_0$ is the difference between the atomic chemical potentials in the supercooled liquid for $T(x,t)$ and T_0. We will put the temperature of the metal to be zero before the beginning of the laser pulse infusion. The temperature distribution after the pulse action can be obtained using the Bio variational principle [see expressions (22)–(27)]. In the linear approximation $T(t) = T_0 - \varepsilon t$, where the cooling rate ε is known. Using the approximation

$$(T_0-\varepsilon t)^{-1} \approx T_0^{-1}(1+\varepsilon t T_0^{-1})$$

and taking into account the fact that $\varepsilon t T_0^{-1} \ll 1$, expression (38) can be rewritten as follows:

$$\frac{\partial r}{\partial t} \approx va\exp\left(-\frac{U}{k_\mathrm{B}T_0}\right)\left[\exp\left(-\frac{U\varepsilon t}{k_\mathrm{B}T_0^2}\right) - \exp\left(-\frac{t\varepsilon}{k_\mathrm{B}T_0^2}\,(h+U)\right)\right]. \quad (39)$$

By integrating Eqn (39), we obtain the time dependence of the nucleus size:

$$r(t) \approx va\exp\left(-\frac{U}{k_\mathrm{B}T_0}\right)\frac{k_\mathrm{B}T_0^2}{\varepsilon U}\left[\frac{h}{h+U} - \exp\left(-\frac{U\varepsilon t}{k_\mathrm{B}T_0^2}\right) + \frac{U}{h+U}\exp\left(-\frac{t\varepsilon}{k_\mathrm{B}T_0^2}\,(h+U)\right)\right].$$

The radius of the nucleus of a crystal during the cooling of the melt with the rate ε tends to its limiting value

$$r_0 \approx va\exp\left(-\frac{U}{k_\mathrm{B}T_0}\right)\frac{k_\mathrm{B}T_0^2}{\varepsilon U}\,\frac{h}{h+U}$$

with the relaxation time $\tau_0 = k_B T_0^2/(\varepsilon U)$, for $U \gg h$. Thus, for $\varepsilon = (10^6 - 10^8)\,^\circ\mathrm{C\ s^{-1}}$, $k_B T/U \approx 0.1$, and $T_0 \approx 10^3\,^\circ\mathrm{C}$, the characteristic time of the process will be $\tau_0 = (10^{-6} - 10^{-4})$ s.

We can linearize equations (27), (29) by averaging the corresponding coefficients of the distribution function $z(n, t)$ derivatives. The diffusion coefficient $D = v \exp(-U/k_B T)\, n^{2/3}$ in the size space depends on two independent variables n and t; therefore, the averaged value is given by

$$\begin{aligned}\langle D\rangle &= \left\langle v \exp\left(-\frac{U}{k_B T}\right) n^{2/3}\right\rangle \\ &= \frac{v}{\tau_0}\int_0^{\tau_0} \exp\left(-\frac{U}{k_B T}\right) \mathrm{d}t\, \frac{1}{n_0}\int_0^{n_0} n^{2/3}\,\mathrm{d}n \\ &= v^3 \exp\left(-\frac{3U}{k_B T_0}\right)\left(\frac{k_B T_0^2}{\varepsilon U}\,\frac{h}{h+U}\right)^2 0{,}6\,[1 - \exp(-1)],\end{aligned}$$

with $n_0 = r_0^3/a^3$, and τ_0 being the characteristic time after which one can neglect the change in the nucleus size. The average value of the driving force equals

$$\left\langle -h\,\frac{T_0 - T(t)}{k_B T_0^2}\right\rangle = -\frac{h\varepsilon}{k_B T_0^2}\,\langle t\rangle = -\frac{h}{2U} = -\alpha\,.$$

After linearization, the set of equations (34)–(37) will take the form

$$\frac{\partial z}{\partial \tau} = \frac{\partial^2 z}{\partial n^2} - \alpha\,\frac{\partial z}{\partial n}\,, \tag{40}$$

$$z(n, 0) = 2N\delta(n-1)\,, \tag{41}$$

$$\left(\frac{\partial z}{\partial n} - \alpha z\right)_{n=1} = 0\,, \tag{42}$$

$$z(\infty, t) = 0\,, \tag{43}$$

where $\tau = \langle D\rangle t$.

By applying the Laplace transformation $L(z) = \varphi(n, s)$ [38] to the set of equations (40)–(43), we obtain

$$\frac{\mathrm{d}^2\varphi}{\mathrm{d}n^2} - \alpha\,\frac{\mathrm{d}\varphi}{\mathrm{d}n} - s\varphi + 2N\delta(n-1) = 0\,, \tag{44}$$

$$\varphi(\infty, s) = 0\,, \tag{45}$$

$$\left(\frac{\mathrm{d}\varphi}{\mathrm{d}n} - \alpha\varphi\right)_{n=1} = 0\,. \tag{46}$$

The solution of the homogeneous equation

$$\frac{\mathrm{d}^2\varphi}{\mathrm{d}n^2} - \alpha\,\frac{\mathrm{d}\varphi}{\mathrm{d}n} - s\varphi = 0$$

assumes the form

$$\varphi = c_1 \exp(k_1 n) + c_2 \exp(k_2 n)\,,$$

where $k_{1,2} = \alpha/2 + \sqrt{\alpha^2/4 + s}$. The unknown functions

$$c_1(n) = \frac{2N\theta(n-1)}{k_2 - k_1}\exp(-k_1) + A\,,$$

$$c_2(n) = \frac{2N\theta(n-1)}{k_2 - k_1}\exp(-k_2) + B\,,$$

where $\theta(n-1)$ is the theta-function:

$$\theta(n-1) = \int_{-\infty}^{n}\delta(n-1)\,\mathrm{d}n = \begin{cases} 0, & n < 1\,,\\ \dfrac{1}{2}\,, & n = 1\,,\\ 1\,, & n > 1\,,\end{cases}$$

can be found by the method of the variation of constants from the equations

$$\frac{\mathrm{d}c_1}{\mathrm{d}n}\exp(k_1 n) + \frac{\mathrm{d}c_2}{\mathrm{d}n}\exp(k_2 n) = 0\,,$$

$$k_1\,\frac{\mathrm{d}c_1}{\mathrm{d}n}\exp(k_1 n) + k_2\,\frac{\mathrm{d}c_2}{\mathrm{d}n}\exp(k_2 n) = -2N\delta(n-1)\,.$$

Constants A and B are determined by boundary conditions (45) and (46):

$$A = \frac{2N\exp(-k_1)}{k_2 - k_1}\,,\quad B = \frac{N}{k_2 - k_1}\left(1 + \frac{k_1 - \alpha}{k_2 - \alpha}\right).$$

As a result, the solution to equation (44) under conditions (45) and (46) will be expressed as follows:

$$\begin{aligned}\varphi(n, s) = {} & \frac{2N\exp\left[k_1(n-1)\right]}{k_2 - k_1}\,\left[\theta(n-1) - 1\right] \\ & + \frac{2N\exp\left[k_2(n-1)\right]}{k_2 - k_1}\left[\theta(n-1) - \frac{k_1 - \alpha}{2(k_2 - \alpha)}\right].\end{aligned}$$

By applying the inverse Laplace transformation $L^{-1}[\varphi(n, s)]$, we find the nucleus size distribution function

$$\begin{aligned}z(n, \tau) = {} & N\exp\frac{\alpha(n-1)}{2}\left\{\frac{1}{\sqrt{\pi\tau}}\exp\left[-\frac{\alpha^2}{4}\,\tau - \frac{(n-1)^2}{4\tau}\right]\right. \\ & \left. - \frac{\alpha}{2}\exp\frac{\alpha(n-1)}{2}\,\mathrm{erfc}\left(\frac{\alpha\sqrt{\tau}}{2} + \frac{n-1}{2\sqrt{\tau}}\right)\right\}.\end{aligned} \tag{47}$$

The derived distribution function, being an approximate solution to the set of equations (39)–(42), is defined for

$$0 \leqslant \tau \leqslant \langle D\rangle\,\tau_0 = \langle D\rangle\,\frac{k_B T_0^2}{\varepsilon U}\,,$$

$$1 < n < n_0 = \frac{4}{3\pi}\left[v\exp\left(-\frac{U}{k_B T_0}\right)\frac{k_B T_0^2}{\varepsilon U}\,\frac{h}{h+U}\right]^3.$$

If the statistical average nucleus size

$$\langle n\rangle = \frac{\int_1^{n_0} z(n, t)\, n\,\mathrm{d}n}{\int_1^{n_0} z\,\mathrm{d}n}$$

is slightly less than the asymptotic size n_0, then n can be assumed to change from 1 to $+\infty$, which holds true either at initial stages of the process or at high cooling rates, $\varepsilon > 10^8$ grad s^{-1}. For large τ ($\tau \gg a^{-2}$), by using the asymptotic representation of $\mathrm{erfc}\,(x) \approx \exp(-x^2)/(\sqrt{\pi}x)$, the distribution function can be written down in the form

$$\begin{aligned}z(n, t) \approx {} & \frac{N\exp\left[(\alpha/2)\,n - n^2/(4\tau) - d^2/(4\tau)\right]}{\sqrt{\pi\tau}} \\ & \times\left[1 - \left(1 + \frac{n}{\alpha\tau}\right)^{-1}\right] = \exp\left(\frac{\alpha n}{2} - \frac{n^2}{4\tau}\right)\varphi(n, \tau)\,.\end{aligned}$$

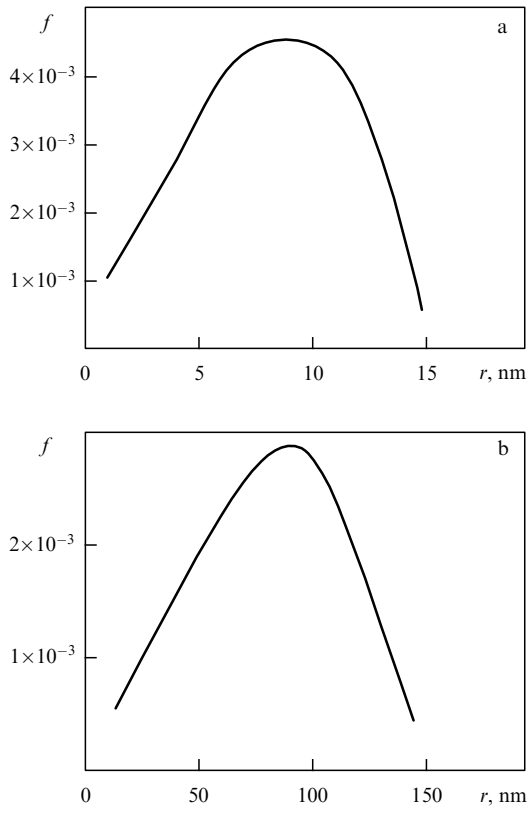

Figure 4. Asymptotic distribution functions for the size of the new phase nuclei, $f = z/N$ (for $\tau = \tau_0\langle D\rangle$), obtained for the cooling rates of (a) $\varepsilon = 10^7$ °C s^{-1}, and (b) $\varepsilon = 10^6$ °C s^{-1}.

Here, the function $\exp\left[\alpha n/2 - n^2/(4\tau)\right]$ has a sharp maximum at $n = \alpha\tau$, but $\varphi(n, \tau)$ changes slowly. Therefore, the extremum of the distribution function $z(n, \tau)$ is situated at the point $n = \langle h\rangle \approx \alpha\tau$. The statistical average size of new phase nuclei depends on the cooling rate as ε^{-3}, because $\tau = \langle D\rangle\,\tau_0 \approx \varepsilon^{-3}$.

Figure 4 plots asymptotic distribution functions for the nucleus size, $f = z/N$ (for $\tau = \tau_0\langle D\rangle$), obtained atr various cooling rates with the following values of the parameters: $U = 1$ eV, $h/U = 0.1$, $k_B T_0 = 0.1$ eV, $v = 10^{12}$ s^{-1}, and $c_p = 30$ J (mol K)$^{-1}$. For the cooling rate $\varepsilon \approx 10^7$ °C s^{-1} (Fig. 4a), the average size of the nuclei is $r \approx 10$ nm. As the cooling rate decreases to 10^6 °C s^{-1} (Fig. 4b), the size distribution function displaces to the right and the nucleus maximum size resides around 100 nm. If $\varepsilon \approx 10^5$ °C s^{-1}, the statistical average nucleus size reaches 500 nm. When the cooling rate is further decreased, a fine-grained crystal structure at the micrometer level is formed. However, it should be noted that the cooling rate estimation was made without taking into account the evaporation and thermal radiation from the melt surface.

5. Conclusion

The development of physical fundamentals for new simple nanostructuring methods (creating surface reliefs with characteristic periods of less than 1 μm on such materials as superhard refractory ceramics, quartz, Teflon, silicon, and polymers) is of great practical interest at the present time. Therefore, it is important to understand the mechanisms and main factors that control the process.

This article presents the experimental and theoretical results obtained by the authors on direct laser nanostructuring of various materials by excimer nanosecond laser pulses. We have analyzed the formation of structures under laser irradiation, the period of which is not connected directly to the radiation wavelength. Direct laser nanostructuring models are being developed for a wide range of technological materials (metals, ceramics) and various surface modification processes — in the presence of surface layer melting and without it.

References

1. Apollonov V V, Prokhorov A M, Shmakov A V, Shmakov V A *Sov. Tech. Phys. Lett.* **17** 59 (1991); *Pis'ma Zh. Tekh. Fiz.* **17** (2) 52 (1991)
2. Shmakov V A *Dokl. Phys.* **52** 470 (2007); *Dokl. Ross. Akad. Nauk* **416** 47 (2007)
3. Khomich V Yu, Shmakov V A *Dokl. Phys.* **57** 349 (2012); *Dokl. Ross. Akad. Nauk* **446** 276 (2012)
4. Tokarev V N et al. *Fiz. Khim. Obrabotki Mater.* (4) 15 (2008)
5. Tokarev V N et al., in *Proc. of the 29th Intern. Congress on Applications of Lasers and Electro-Optics, Anaheim, CA, 2010*, p. 1257
6. Makarov G N *Phys. Usp.* **56** 643 (2013); *Usp. Fiz. Nauk* **183** 673 (2013)
7. Keilmann F, Bai Y H *Appl. Phys. A* **29** 9 (1982)
8. Aksenov V P, Zhurkin B G *Sov. Phys. Dokl.* **27** 630 (1982); *Dokl. Akad. Nauk SSSR* **265** 1365 (1982)
9. van Driel H M, Sipe J E, Young J F *Phys. Rev. Lett.* **49** 1955 (1982)
10. Bonch-Bruevich A M et al. *Izv. Akad. Nauk SSSR Fiz.* **46** 1186 (1982)
11. Fauchet P M, Siegman A E *Appl. Phys. Lett.* **40** 824 (1982)
12. Samokhin A A, Sychugov V A, Tishchenko A V *Sov. J. Quantum Electron.* **13** 1433 (1983); *Kvantovaya Elektron.* **10** 2139 (1983)
13. Anisimov V N, Baranov V Yu, Bolshov L A *Poverkhnost* (7) 138 (1983)
14. Akhmanov S A et al. *Sov. Phys. Usp.* **28** 1084 (1985); *Usp. Fiz. Nauk* **147** 675 (1985)
15. Siegman A E, Fauchet P M *IEEE J. Quantum Electron.* **22** 1384 (1986)
16. Bolle M, Lazare S *J. Appl. Phys.* **73** 3516 (1993)
17. Dyer P E, Jenkins S D, Sidhu J *Appl. Phys. Lett.* **52** 1880 (1988)
18. Niino H et al. *Appl. Phys. Lett.* **55** 510 (1989)
19. Zheleznov Yu A et al. *Prikladnaya Fiz.* (3) 83 (2014)
20. Zheleznov Yu A et al. *Pis'ma Mater.* **4** 45 (2014)
21. Lapshin K E et al. *Fiz. Khim. Obrabotki Mater.* (1) 43 (2008)
22. Nebogatkin S V et al., in *8th Intern. Conf. on Nanosciences & Nanotechnologies, Thessaloniki, Greece, 2011, Abstract Book*, p. 302
23. Mandelshtam L I, Leontovich M A *Zh. Eksp. Teor. Fiz.* **7** 817 (1937)
24. Leontovich M A *Vvedenie v Termodinamiku* (Introduction to the Thermodynamics) 2nd ed. (Moscow–Leningrad: GITTL, 1952)
25. Gaponov-Grekhov A V et al. *Nelineinye Volny*: *Dinamika i Evolyutsiya* (Nonlinear Waves: Dynamics and Evolution) (Exec. Eds A V Gaponov-Grekhov, M I Rabinovich) (Moscow: Nauka, 1989) p. 61
26. Shilov G E *Mathematical Analysis* Vol. 1 (Cambridge, Mass.: MIT Press, 1973); Translated from Russian: *Matematicheskii Analiz. Konechnomernye Lineinye Prostranstva* (Moscow: Nauka, 1969)
27. Haken H *Advanced Synergetics*: *Instability Hierarchies of Self-Organizing Systems and Devices* (Berlin: Springer-Verlag, 1983); Translated into Russian: *Sinergetika*: *Ierarkhiya Neustoichivostei v Samoorganizuyushchikhsya Sistemakh i Ustroistvakh* (Moscow: Mir, 1985)
28. Ganin D V et al. *Quantum Electron.* **44** 317 (2014); *Kvantovaya Elektron.* **44** 317 (2014)
29. Khomich V Yu et al. *Fiz. Khim. Obrabotki Mater.* (6) 15 (2012)
30. Zeldovich Ya B *Zh. Eksp. Teor. Fiz.* **12** 525 (1942)
31. Biot M A *Variational Principles in Heat Transfer*: *A Unified Lagrangian Analysis of Dissipative Phenomena* (Oxford: Clarendon

Press, 1970); Translated into Russian: *Variatsionnye Printsipy v Teorii Teploobmena. Unifitsirovannyi Analiz Dissipativnykh Yavlenii Metodom Lagranzha* (Moscow: Energiya, 1975)
32. Christian J W *The Theory of Transformations in Metals and Alloys* 2nd ed. (Oxford: Pergamon Press, 1975); Translated into Russian: *Teoriya Prevrashchenii v Metallakh i Splavakh* (Moscow: Mir, 1978)
33. Khomich V Yu, Shmakov V A *Dokl. Phys.* **56** 309 (2011); *Dokl. Ross. Akad. Nauk* **438** 460 (2011)
34. Mikolutskii S I et al. *Usp. Priklad. Fiz.* **1** 548 (2013)
35. Lapshin K E et al. *Ross. Nanotekhnol.* **2** (11 – 12) 50 (2007)
36. Tokarev V N et al. *Dokl. Phys.* **53** 206 (2008); *Dokl. Ross. Akad. Nauk* **419** 754 (2008)
37. Chandrasekhar S *Rev. Mod. Phys.* **15** 1 (1943); Translated into Russian: *Stokhasticheskie Problemy v Fizike i Astronomii* (Moscow: IL, 1947)
38. Ditkin V A, Prudnikov A P *Spravochnik po Operatsionnomu Ischisleniyu* (Handbook of Operational Calculation) (Moscow: Vysshaya Shkola, 1965)